Biochemical and Biophysical Research Communications 570 (2021) 82–88

Contents lists available at ScienceDirect

Biochemical and Biophysical Research Communications

journal homepage: www.elsevier.com/locate/ybbrc

Rapid protein delivery to living cells for biomolecular investigation

Francesco Torricella [a], Alessio Bonucci [b, 1], Panagis Polykretis [c, 1], Francesca Cencetti [d], Lucia Banci [a, c, e, *]

[a] Magnetic Resonance Center - CERM, University of Florence, via Luigi Sacconi 6, 50019, Sesto Fiorentino, Florence, Italy
[b] Aix Marseille, Univ, CNRS, BIP, Laboratoire de Bioénergétique et Ingégnerie des protéines, Marseille, France
[c] Interuniversity Consortium for Magnetic Resonance of Metallo Proteins (CIRMMP), via Luigi Sacconi 6, 50019, Sesto Fiorentino, Florence, Italy
[d] Department of Experimental and Clinical Biomedical Sciences "Mario Serio", University of Florence, v.le GB Morgagni 50, 50134, Florence, Italy
[e] Department of Chemistry, University of Florence, via della Lastruccia 3, 50019, Sesto Fiorentino, Florence, Italy

ARTICLE INFO

Article history:
Received 1 July 2021
Accepted 4 July 2021
Available online 15 July 2021

Keywords:
Protein delivery
In-cell EPR
Thermal vesiculation
Structural biology
Protein dynamic

ABSTRACT

The lack of a simple, fast and efficient method for protein delivery is limiting the widespread application of in-cell experiments, which are crucial for understanding the cellular function. We present here an innovative strategy to deliver proteins into both prokaryotic and eukaryotic cells, exploiting thermal vesiculation. This method allows to internalize substantial amounts of proteins, with different molecular weight and conformation, without compromising the structural properties and cell viability. Characterizing proteins in a physiological environment is essential as the environment can dramatically affect the conformation and dynamics of biomolecules as shown by in-cell EPR spectra vs those acquired in buffer solution. Considering its versatility, this method opens the possibility to scientists to study proteins directly in living cells through a wide range of techniques.

1. Introduction

The complete description and deep understanding of the cellular functional processes at the basis of life requires a molecular approach which can decipher the various functions in detail and rationalize their impairments, caused by mutations and/or altered physiological states. On the other hand, the high-resolution atomic level characterization needs to be performed at cellular level, in order to maintain all the physiological conditions and the complexity of the environment in which each cellular component operates. Several methods have been implemented which allow the detailed description of proteins and of the pathways in which they are involved within living cells, including monitoring the effects of oxidative stress, the addition of small molecules and drugs, as well as their interactions [1] and the occurrence of functional processes. One of the most effective techniques is in-cell NMR, where, through transient transfection, proteins have been directly expressed and analyzed in living cells [2–4]. Such technique allowed us to study various protein processes such as interactions, the effects of cofactors and the exposure to drugs [5–8]. However, this approach is not suitable for some techniques such as EPR or FRET, since labelling reactions are effectively performed before protein insertion in the cells [9,10]. Up to now the main method for the internalization of proteins is bulk electroporation [11], in which an external electric field increases the permeability of cell membranes [12–15]. Nevertheless, the high voltage input inevitably causes critical temperature increments, pH variations, and the formation of reactive oxygen species, which can affect protein folding and damage cells [16]. Other strategies, such as cell penetrating peptides, pore-forming toxins or nanoparticles, and the mechanical insertion of biomolecules in *Xenopus laevis* oocytes, require specific skills and/or a conspicuous amount of work for sample preparation [16–23]. Recently, through genetic encoding of noncanonical amino acids, it has been described the possibility to perform in-cell EPR distance measurements by overexpressing the protein of interest in bacterial cells and successively grafting the paramagnetic tag, exploiting the permeability of the spin label [24,25]. Such method has been also employed to perform in-cell FRET experiments [26]. However, the success of this approach strongly depends on the intrinsic expression properties of each protein, and requires a demanding co-transfection with the plasmid expressing the gene of interest and with a second one that contains the orthogonal tRNA and aminoacyl-tRNA synthetase specific for an unnatural amino

* Corresponding author. Magnetic Resonance Center - CERM, University of Florence, via Luigi Sacconi 6, 50019, Sesto Fiorentino, Florence, Italy.
E-mail address: banci@cerm.unifi.it (L. Banci).
[1] These authors contributed equally to this work.

https://doi.org/10.1016/j.bbrc.2021.07.006

acid [27].

Thermal vesiculation is used for the delivery of nucleic acids into bacterial competent cells (commonly known as transformation), since 1972 [28]. Despite this strategy is routinely applied for DNA transformation into bacteria, thermal treatments have never been employed to deliver macromolecules, such as proteins, into bacteria and yeast cells [29]. In this work, we applied this long-standing and common technique for a new application, that is the delivery of proteins into both prokaryotic and eukaryotic cells. We found that a treatment close to physiological temperature (42 °C) allows to internalize different types of proteins into bacteria and yeasts. Through the use of confocal fluorescent microscopy, we initially assessed the proper effectiveness of heat-shock protein, verifying the insertion of enhanced green fluorescent protein (EGFP) and of human ubiquitin (Ub) labelled with the atto-488 maleimido (Merck) fluorescent tag. Together with confocal microscopy, continuous wave (cw)-EPR spectroscopy in combination with Site Directed Spin Labeling (SDSL) was used as method to probe the correct delivery. The insertion protocol here presented was therefore tested on proteins up to 30 kDa (Fig. 1a) with different conformational properties indicating that the approach here presented has the potentialities to be used to study a wide variety of systems. All cw-EPR spectra recorded for the in-cell samples showed clear differences in terms of conformation and dynamics compared to those acquired *in vitro*, evidencing the importance of performing experiments in living cells.

2. Material and Methods

Heat shock insertion protocol. For bacterial cells we used 50 μL of 1 mM EGFP solution in PBS buffer pH 7.4 (Gibco®) to resuspend a pellet containing approximately 10^9 cells/mL *E. coli* DH5α competent cells. Then, the cells were incubated at 42 °C for 1 min to induce the vesiculation and thus the internalization of the external protein (Fig. 1b). The cells were then washed 4 times with isotonic phosphate buffer to remove the EGFP which was not internalized into bacteria.

P. pastoris X-33 cells, previously stored in BEDS solution, were incubated at 30 °C for 10 min. The cells were then centrifuged at 2800 g for 3 min and then resuspended in 50 μL of TE buffer supplemented with 0.1% v/v lithium acetate. Then, 1 mM EGFP solution was added to 2 x 10^8 cells/mL *P. pastoris* X-33 cells. The yeast cells were finally incubated at 42 °C for 10 min to promote the protein internalization (Fig. 1c). The cells were then centrifuged, the protein solution was removed and the pellet was washed four times with isotonic PBS buffer. We selected the optimal experimental condition using different concentrations of spin labelled Ub, ranging from 250 μM to 1 mM (Fig. S4). For the in-cell cw-EPR experiments the external protein concentration of 1 mM was selected for both, *E. coli* and *P. pastoris* cells, in order to obtain a good spectral S/N ratio. The supernatant solution of each wash step was checked by EPR to assure the complete removal of the not-internalized spin labelled protein.

Protein purification and cw-EPR experimental procedure. A detailed description of the protein expression and purification as

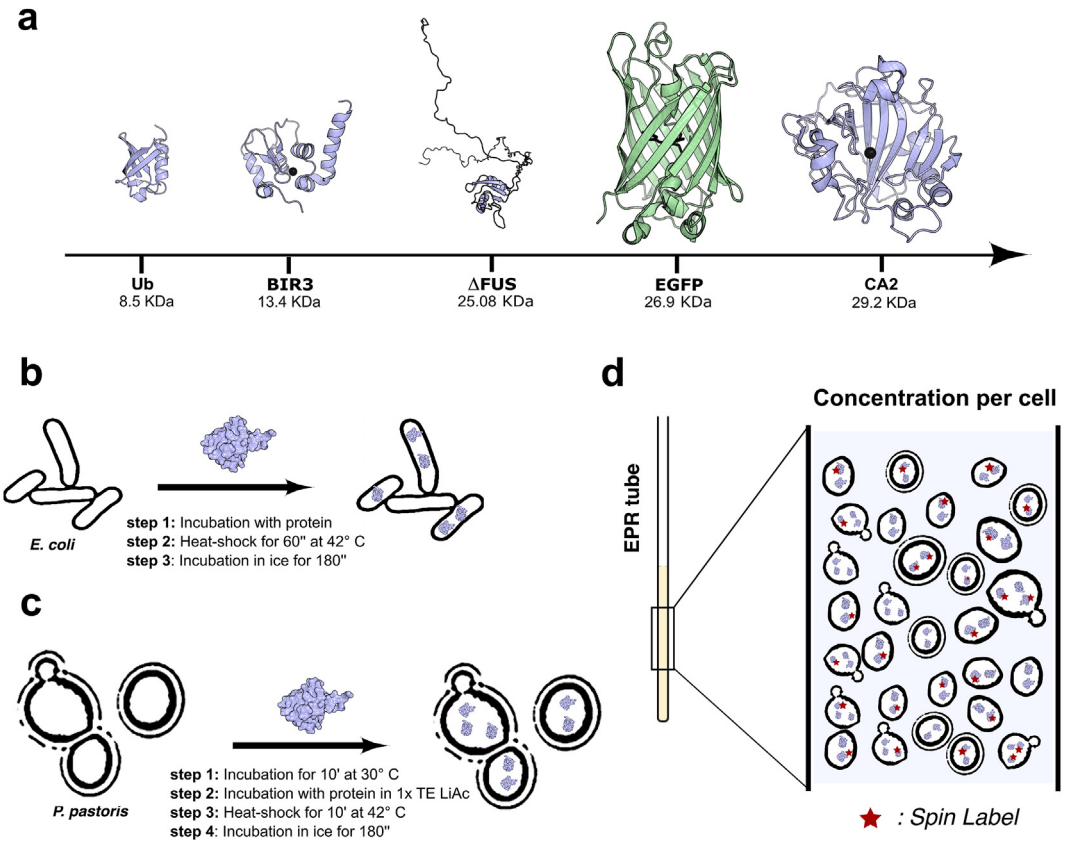

Fig. 1. (a) PDB Structures of the proteins used in this study (Ub:1ubq; BIR3: 6ey2; ΔFUS: modelled structure; EGFP: 2Y0G; CA2: 3ks3) showing their structural conformation and molecular weight. (b) Graphical representation of the delivery into bacterial and (c) yeast cells. d) Schematic representation of protein internalization and of spin labelled protein fraction.

well as of the protein spin labelling for cw-EPR experiments is described in the Supplementary Material (see section 1 and 2).

3. Results and discussion

Transformation is a widely used technique in Molecular Biology for the internalization of circular DNA in *E. coli* cells, in which vesiculation is induced by a heat-shock cycle at 42 °C for a defined amount of time (usually 45–60 s). Similarly, the internalization of extracellular molecules is stimulated in *P. pastoris* when cells are incubated at external temperatures ranging from 40 to 45 °C [31]. The heat-shock procedure here presented (Fig. 1b–d), exploits this behavior of bacteria and yeast cells for delivering proteins into their intracellular environment [32,33], suitable for molecular and structural investigation. The efficacy of the heat-shock procedure and the relative localization of the delivered proteins were checked by monitoring the internalization of EGFP and of atto488-Ub into *E. coli* DH5α and *P. pastoris* X-33 cells. Confocal microscopy assessed the delivery of both proteins into the cell and clearly showed that the vast majority of the protein molecules are localized in the cytoplasm, without affecting the viability and morphology of both bacteria and yeasts for a time up to 120 min (Fig. 2, **4e** and **f**). Indeed, the observed budding of yeasts is a clear evidence of the health status of the cells.

The first crucial aspect for the applicability of the heat-shock procedure is the thermal stability of the proteins to an external temperature of 42 °C, for a period ranging from 1 to 10 min. To test this, Circular Dichroism (CD) spectra were acquired at different temperatures, revealing that all selected proteins are not thermally denatured in our experimental conditions (Supplementary Materials, Fig. S1). We then applied cw-EPR spectroscopy coupled with site directed spin labelling (SDSL) to assess the feasibility of this method of protein internalization for in-cell experiments. The SDSL-EPR spectroscopy generally relies on the attachment of a spin label, such as a nitroxide radical, onto a cysteine residue, for the characterization of the conformation and dynamics of the protein region where it is attached [34–37]. In general, sharp EPR signals of nitroxide-labelled proteins are due to high flexibility of the system (short τ_c values), while broad lines correspond to reduced mobility (long τ_c values) [34]. In our EPR experiments, the 3-maleimido Proxyl (ma-Px) radical was selected as nitroxide paramagnetic probe, since it revealed a good resistance to bio-reduction inside living cells for the time interval necessary to perform cw-EPR measurements at room temperature (Supplementary Materials, Fig. S2). In fact, the typical EPR spectrum arising from a conjugated nitroxide moiety on the ΔFUS disordered region remains up to 35–40 min after the post-delivery preparation time of around 10 min. Despite previous works reported that the nitroxide moiety present in the ma-Px is prone to bio-reduction under *in vitro* conditions [38,39], recent data showed that the same moiety, attached to the non-canonical amino acid para-ethynyl-phenylalanine (pENF) remains stable for approximately 120 min in the bacterial cytoplasm after the addition of azido-proxyl spin label, thus making possible the acquisition of cw and pulsed EPR data [24]. Therefore, our internalization method, which allows to start data acquisition after a short period of time, offers a significant advantage when using spin labels prone to bio-reduction and extends the applicability of the stable ones [13,40].

To test our approach, we selected four different proteins with different molecular weights (ranging from 13.4 to 29.2 kDa) and conformations (from globular to disordered). Specifically, we used the globular baculoviral IAP repeat domain (BIR3) of the X-chromosome linked inhibitor of apoptosis protein (XIAP), the disordered fused in sarcoma protein (ΔFUS a.a. 165–422 [30]) and the globular and folded human carbonic anhydrase 2 (CA2) (Fig. 1a). Each protein was labelled with ma-Px on native cysteines (BIR3 and CA2) or selectively introduced ones (Ub and ΔFUS). Proteins were then internalized in *E. coli* cells through the heat-shock protocol (see Supplementary Materials section 1 and 2 and Material and Methods). The external concentration of 1 mM was selected to gain the best spectral S/N ratio (Supplementary Materials, Fig. S4). The efficiency of the procedure was estimated using a standard calibration curve made of samples of known concentrations of ma-Px (Fig. 3b). The labelling efficiency of each protein depends on the

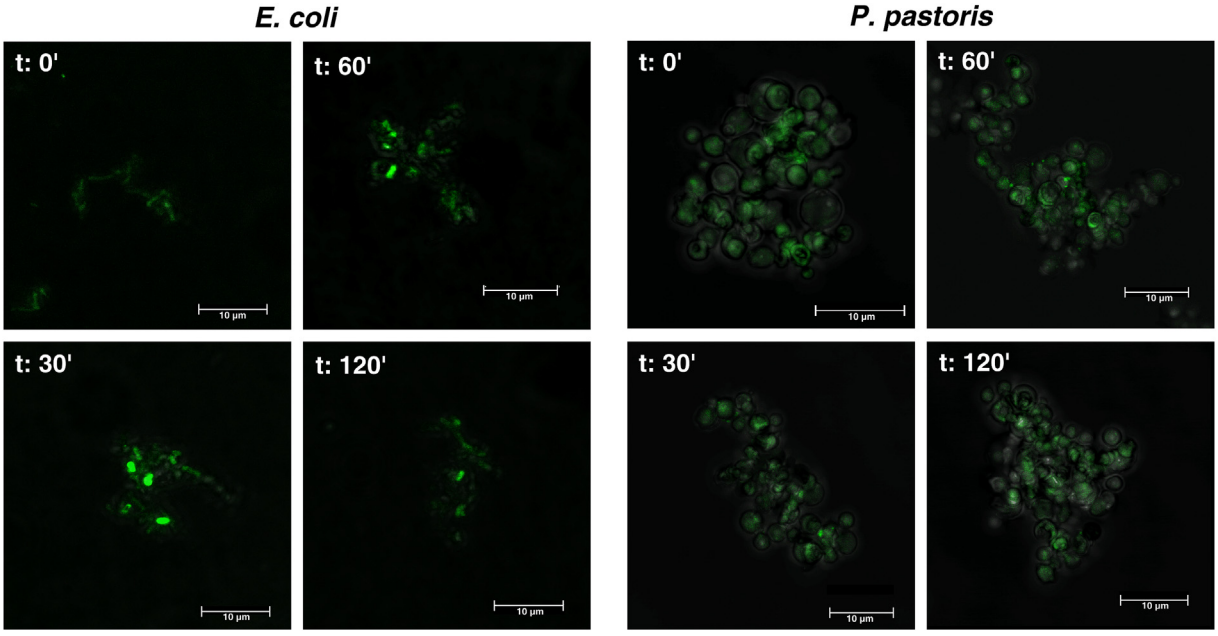

Fig. 2. Confocal microscopy images acquired at different times and on different cellular fields after the delivery of EGFP into *E. coli* and *P. pastoris* (t: 0′ corresponds to the first acquisition after the preparation of the cell samples with a dead time of ~10 min). The images were obtained by merging bright and fluorescence fields (see Supporting information Fig. S6).

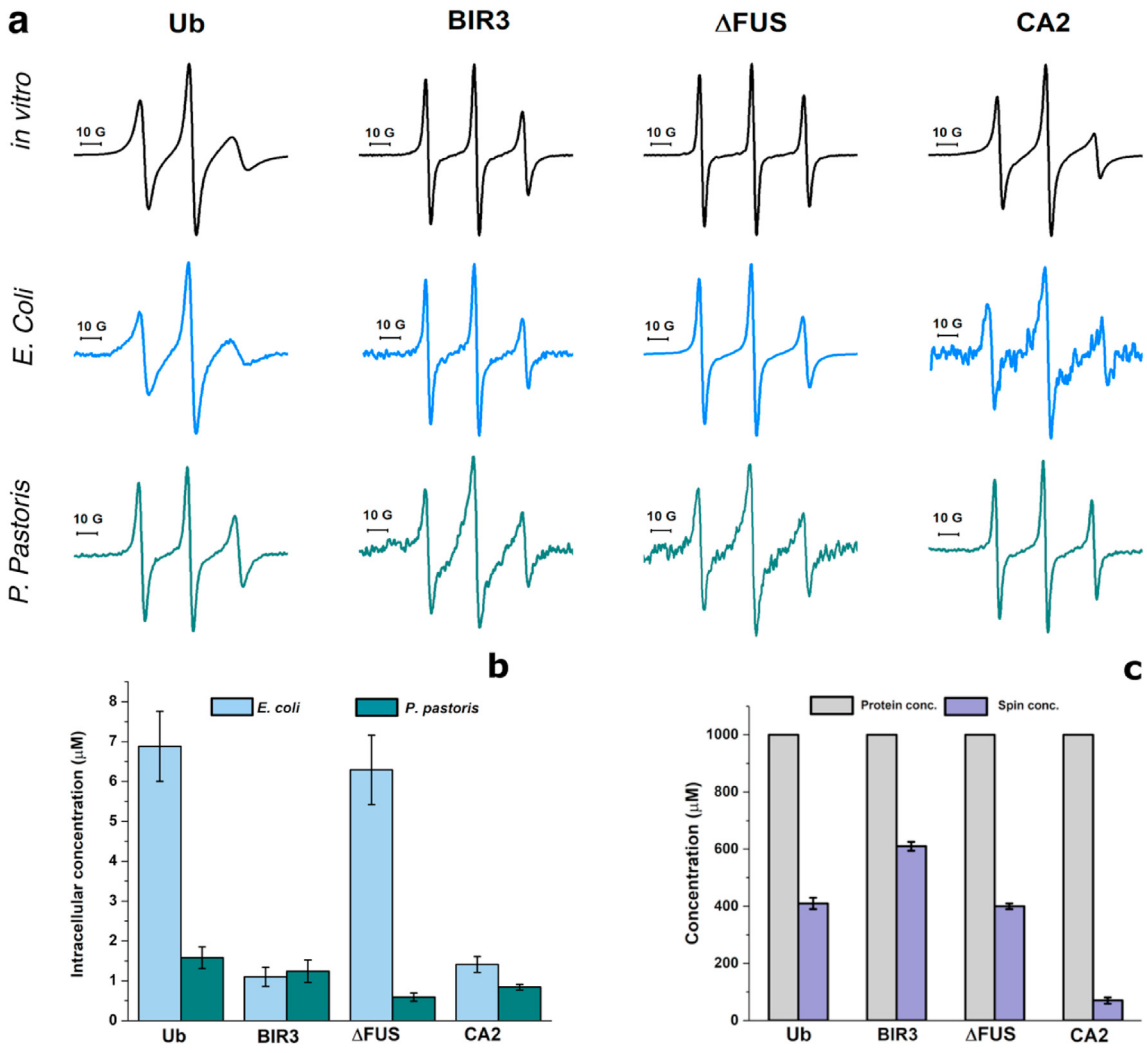

Fig. 3. (a) cw-EPR (X-band) spectra of Ub, BIR3, ΔFUS and CA2 acquired *in vitro*, in *E. coli* and in *P. pastoris* at 298 K. (b) Estimate of the intracellular labelled protein concentrations based on the in-cell cw-EPR double integral. Each concentration value was derived using a standard calibration curve determined on a ma-Px sample at know concentrations, and repeating the measurement three times. (c) Effective yield of the spin labelling reaction on the free cysteine residues of the analyzed proteins (Ub: ~41%, BIR3: ~61%, ΔFUS: ~43%, CA2: ~7%).

labelling protocol combined with the exposure of the target cysteine to the solvent. Indeed, the labelling efficiency of CA2 resulted particularly low since its labelling site is buried within the protein structure (Fig. 3c).

For Ub, BIR3 and ΔFUS In *E.coli* cells (Fig. 3a), we detected broader cw- EPR at X-band frequency (9.8 GHz) signals, with longer τ_c than those observed in the spectra acquired *in vitro* (Table 1), indicating a decrease in mobility of the proteins once located in the bacterial cytoplasm. In fact, the line-shape of the cw-EPR spectra recorded *in vitro* at X-band frequency (9.8 GHz) resulted different for each protein, since they depend on the dynamics of the ma-Px labelling position (Fig. 3a). The analysis performed *in vitro* and the spectra simulation (Supplementary Materials, Fig. S3) assessed the intrinsically disordered behavior of the spin labelled region of ΔFUS, the mobility for BIR3 (in the range of 0.4–1.5 ns) and the more compact conformation of Ub and CA2. Our results showed that these proteins can be effectively internalized in the cell. They also indicated that, even though the prokaryotic intracellular environment is different with respect to the eukaryotic one, it can affect protein internal mobility gaining fundamentals information that can be coupled with the standard *in vitro* approach. Contrarily, the EPR spectrum and the relative parameters of CA2 in bacterial cells resulted very similar to those *in vitro*, suggesting that the conformation and dynamics of this protein are not altered in bacteria.

To extend the protocol to eukaryotic cells, we selected the wild-type X-33 strain of *P. Pastoris* and we analyzed the same set of labelled proteins which were employed for confocal microscopy and cw-EPR measurements in bacteria (Fig. 1c). From cw-EPR spectra we estimated the labelled protein concentrations inside *P. pastoris* cells to be in the range of 0.5–1.5 μM (Fig. 3b) and for *E. coli* cells to be in the range of 1.2–6.8 μM. These values represent the concentration in the relative living systems right after the delivery time and the preparation dead time that is in the range of 10–12 min (see Materials and Methods). Specifically, through in-gel fluorescence the total concentration of internalized atto488-Ub was roughly estimated to be ~1.7 μM in bacteria and ~3.3 μM in yeasts (Fig. 4g), while through Western Blot analysis the total concentration of internalized BIR3 was estimated to be ~4.9 μM in bacteria and ~1.8 μM in yeasts (Supplementary Materials, Fig. S5). Considering these results, our protocol allows to internalize levels of proteins inside bacteria and yeasts, sufficient for providing EPR data with an acceptable S/N ratio.

Our in-cell cw-EPR results showed that BIR3 and ΔFUS inside yeast cells displayed different spectral lineshapes compared to

Table 1
Correlation time values and spectral components of the *in vitro* and in-cell measurements, obtained from the simulation of the experimental data (the simulations were performed by the EasySpin package [42]).

	1st Component tc (ns)	1st Component Percentage (%)	2st Component tc (ns)	2st Component Percentage (%)
Ub (*in vitro* at 20 mW)	1.04	100	–	–
Ub (*in vitro* at 126 mW)	0.42	100	–	–
Ub (*E. coli* at 20 mW)	0.94	42.0	3.89	58.0
Ub (*P. pastoris* at 126 mW)	0.32	79.0	0.47	21.0
BIR3 (*in vitro* at 20 mW)	0.40	46.7	1.49	53.3
BIR3 (*in vitro* at 126 mW)	0.23	70	1.03	30
BIR3 (*E. coli* at 20 mW)	0.30	38.0	2.04	62.0
BIR3 (*P. pastoris* at 126 mW)	0.30	16.6	4.24	83.4
ΔFUS (*in vitro* at 20 mW)	0.16	100	–	–
ΔFUS (*in vitro* at 126 mW)	0.16	100	–	–
ΔFUS (*E. coli* at 20 mW)	0.27	58.0	1.46	42.0
ΔFUS (*P.pastoris* at 126 mW)	0.27	25.2	3.16	74.8
CA2 (*in vitro* at 20 mW)	0.40	31.6	1.74	68.4
CA2 (*in vitro* at 126 mW)	0.35	38.2	1.74	61.8
CA2 (*E. coli* at 20 mW)	0.35	26.5	1.84	73.5
CA2 (*P. pastoris* at 126 mW)	0.14	37.4	1.75	62.6

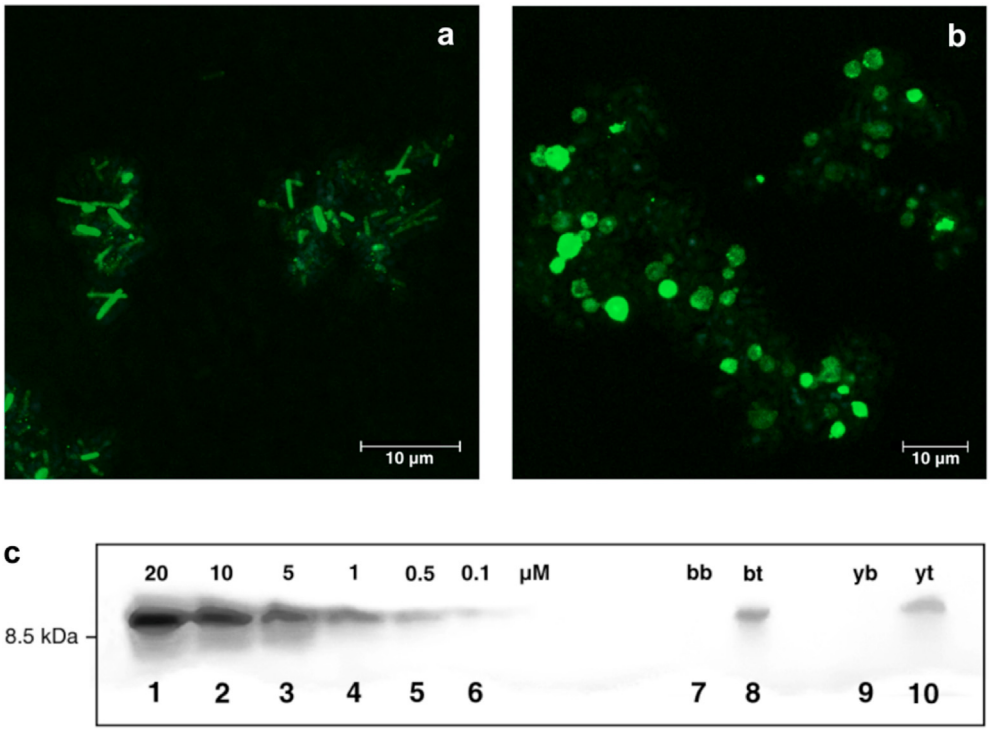

Fig. 4. Confocal microscopy images, obtained merging bright and fluorescent fields of *E. coli* (a) and *P. pastoris* (b) after the delivery of atto488-Ub. (c) in-gel fluorescence of atto488-Ub excited at 501 nm: Lane 1) atto488-Ub 20 μM; lane 2) 10 μM; lane 3) 5 μM; lane 4) 1 μM; lane 5) 0.5 μM; lane 6) 0.1 μM; lane 7) control *E. coli* lysate; lane 8) treated *E. coli* lysate; lane 9) control *P. pastoris* lysate; lane 10) treated *P. pastoris* lysate.

those obtained *in vitro* and in *E. coli* (Fig. 3a). The broad component indicative of slower motions (with ~3–4 μs of τ_c values and 74.8% and 83.4% of the total EPR signal for BIR3 and ΔFUS, respectively) dominates the spectra, indicating that the physiological conditions of the eukaryotic cells induce a drastic reduction of the dynamics of both proteins.

Surprisingly, the EPR spectrum of Ub inside *P. pastoris* cells features two distinct sharp components with different percentages and fast tumbling rates (0.32 ns and 0.47 ns respectively, see Table 1), suggesting that inside eukaryotic cells Ub possesses highly dynamic conformations for the region surrounding the spin label, notably different from those acquired *in vitro* and in bacterial cells. A less evident effect was observed for CA2 in yeast cells. The CA2 in-cell EPR spectrum is mainly composed by a broad signal with the same τ_c (1.75 ns) as that determined for the *in vitro* sample, while the minor component indicates a faster tumbling motion compared to that observed *in vitro*. Such peculiar increased dynamics observed for Ub and CA2 could be related to intracellular proteolytic events. To address this hypothesis, we acquired cw-EPR spectra on Ub after incubating the protein with a mixture of proteases (Supplementary Materials, Fig. S6). Such experiment evidenced an actual increment of the τ_c of Ub *in vitro* in absence of

protease inhibitor, suggesting that the increment of τ_c observed in cell could be due to proteolytic activity.

Our results prove that the overall efficacy of the method does not depend on the structural properties of the proteins used in this study and, more importantly, that it does not alter their structure. As shown the levels of internalized protein are such that our protocol could be suitable for several types of experiments, as pulsed-EPR in living cells, in-cell FRET, in-cell NMR, cell tomography and various microscopies. Indeed, a recent work reported the possibility to perform pulsed EPR PELDOR/DEER measurements either in solution or in-cell, at this levels of protein concentration [41]. Confocal microscopy confirmed that the internalized EGFP and the atto488-Ub were uniformly distributed in the cytoplasm and did not cause any observable cytotoxicity, since both bacteria and yeasts are viable even 120 min after the internalization. The cw-EPR data confirmed the importance of performing protein characterization directly into living systems, gaining more detailed and physiological information about the structure and the dynamics of proteins. Notably, all proteins selected in this study reported remarkable differences in their dynamics between *in vitro* and in-cell experiments. In conclusion, in this work we present a new, simple and versatile protein internalization method, which does not require expensive instrumentation or specific training and which can effectively complement those already available, thus implementing the possibility to perform molecular and structural investigation experiments in living cells. This work therefore represents an innovative approach which has extensive potentialities for further improvement in terms of internalization efficiency and applicability.

Author contributions

F.T. and L.B. conceived the work; F.T., A.B. and P.P. designed the experiments; F.T., A.B. and P.P., produced the protein samples; F.T. and A.B. performed the EPR experiments and analyzed the data; F.C. performed the confocal microscopy experiments; P.P. performed the Western Blot analysis; F.T., A.B., P.P. and L.B. wrote the manuscript.

Declaration of competing interest

The authors declare no competing interests.

Acknowledgements

This work has been supported by EC H2020 projects iNEXT-Discovery (n. 871037) and Instruct-ULTRA (n. 731005). The authors acknowledge the support and the use of resources of Instruct-ERIC, an ESFRI Landmark, and specifically the CERM/CIRMMP Italy Centre. AB is grateful to Regione Toscana for a post-doctoral grant (POR-FSE 2014–2020). The confocal microscopy data was in part acquired with the equipment of the “Medicina Molecolare” Facility, funded by MIUR, Bando Dipartimenti di Eccellenza 2018–2022”.

Appendix A. Supplementary data

Supplementary data to this article can be found online at https://doi.org/10.1016/j.bbrc.2021.07.006.

References

[1] S.L. Speer, et al., The intracellular environment affects protein-protein interactions, Proc. Natl. Acad. Sci. U. S. A. 118 (11) (2021).
[2] E. Luchinat, L. Banci, In-cell NMR in human cells: direct protein expression allows structural studies of protein folding and maturation, Acc. Chem. Res. 51 (6) (2018) 1550–1557.
[3] E. Luchinat, L. Banci, A unique tool for cellular structural Biology: in-cell NMR, J. Biol. Chem. 291 (8) (2016) 3776–3784.
[4] E. Luchinat, L. Banci, In-cell NMR: a topical review, IUCrJ 4 (Pt 2) (2017) 108–118.
[5] P. Polykretis, et al., Cadmium effects on superoxide dismutase 1 in human cells revealed by NMR, Redox Biol 21 (2019) 101102.
[6] E. Luchinat, et al., Drug screening in human cells by NMR spectroscopy allows the early assessment of drug potency, Angew Chem. Int. Ed. Engl. 59 (16) (2020) 6535–6539.
[7] L. Banci, et al., Atomic-resolution monitoring of protein maturation in live human cells by NMR, Nat. Chem. Biol. 9 (5) (2013) 297–299.
[8] M.J. Capper, et al., The cysteine-reactive small molecule ebselen facilitates effective SOD1 maturation, Nat. Commun. 9 (1) (2018) 1693.
[9] A. Bonucci, et al., In-cell EPR: progress towards structural studies inside cells, Chembiochem 21 (4) (2020) 451–460.
[10] S. Padilla-Parra, M. Tramier, FRET microscopy in the living cell: different approaches, strengths and weaknesses, Bioessays 34 (5) (2012) 369–376.
[11] F.X. Theillet, et al., Structural disorder of monomeric alpha-synuclein persists in mammalian cells, Nature 530 (7588) (2016) 45–50.
[12] A. Dalaloyan, et al., Tracking conformational changes in calmodulin in vitro, in cell extract, and in cells by electron paramagnetic resonance distance measurements, ChemPhysChem 20 (14) (2019) 1860–1868.
[13] Y. Yang, et al., In-cell trityl–trityl distance measurements on proteins, J. Phys. Chem. Lett. 11 (3) (2020) 1141–1147.
[14] T. Kotnik, et al., Membrane electroporation and electropermeabilization: mechanisms and models, Annu. Rev. Biophys. 48 (2019) 63–91.
[15] Y. Yang, et al., In-cell destabilization of a homodimeric protein complex detected by DEER spectroscopy, Proc. Natl. Acad. Sci. U. S. A. 117 (34) (2020) 20566–20575.
[16] C. Chau, P. Actis, E. Hewitt, Methods for protein delivery into cells: from current approaches to future perspectives, Biochem. Soc. Trans. 48 (2) (2020) 357–365.
[17] H. Barth, et al., The binary Clostridium botulinum C2 toxin as a protein delivery system: identification of the minimal protein region necessary for interaction of toxin components, J. Biol. Chem. 277 (7) (2002) 5074–5081.
[18] P. Selenko, et al., Quantitative NMR analysis of the protein G B1 domain in Xenopus laevis egg extracts and intact oocytes, Proc. Natl. Acad. Sci. U. S. A. 103 (32) (2006) 11904–11909.
[19] R. Igarashi, et al., Distance determination in proteins inside Xenopus laevis oocytes by double electron-electron resonance experiments, J. Am. Chem. Soc. 132 (24) (2010) 8228–8229.
[20] A. Dinca, W.M. Chien, M.T. Chin, Intracellular Delivery of Proteins with cell-penetrating Peptides for therapeutic Uses in human disease, Int. J. Mol. Sci. 17 (2) (2016) 263.
[21] Y.W. Lee, et al., Protein delivery into the cell cytosol using non-viral nanocarriers, Theranostics 9 (11) (2019) 3280–3292.
[22] A. Collauto, et al., Compaction of RNA duplexes in the cell*, Angew Chem. Int. Ed. Engl. 59 (51) (2020) 23025–23029.
[23] H.B. Schmidt, R. Rohatgi, *In* vivo formation of vacuolated multi-phase compartments lacking membranes, Cell Rep. 16 (5) (2016) 1228–1236.
[24] P. Widder, et al., Combining site-directed spin labeling in vivo and in-cell EPR distance determination, Phys. Chem. Chem. Phys. 22 (9) (2020) 4875–4879.
[25] S. Kucher, et al., In cell Gd(3+)-based site-directed spin labeling and EPR spectroscopy of eGFP, Phys. Chem. Chem. Phys. 22 (24) (2020) 13358–13362.
[26] S.-H. Park, et al., Analysis of protein–protein interaction in a single live cell by using a FRET system based on genetic code expansion technology, J. Am. Chem. Soc. 141 (10) (2019) 4273–4281.
[27] M.R. Fleissner, D. Cascio, W.L. Hubbell, Structural origin of weakly ordered nitroxide motion in spin-labeled proteins, Protein Sci. 18 (5) (2009) 893–908.
[28] S.N. Cohen, A.C. Chang, L. Hsu, Nonchromosomal antibiotic resistance in bacteria: genetic transformation of Escherichia coli by R-factor DNA, Proc. Natl. Acad. Sci. U. S. A. 69 (8) (1972) 2110–2114.
[29] M.P. Stewart, R. Langer, K.F. Jensen, Intracellular delivery by membrane disruption: mechanisms, strategies, and concepts, Chem. Rev. 118 (16) (2018) 7409–7531.
[30] A. Bonucci, et al., A combined NMR and EPR investigation on the effect of the disordered RGG regions in the structure and the activity of the RRM domain of FUS, Sci. Rep. 10 (1) (2020) 20956.
[31] R.D. Gietz, R.H. Schiestl, Large-scale high-efficiency yeast transformation using the LiAc/SS carrier DNA/PEG method, Nat. Protoc. 2 (1) (2007) 38–41.
[32] S. Ghaemmaghami, et al., Global analysis of protein expression in yeast, Nature 425 (6959) (2003) 737–741.
[33] Y. Ishihama, et al., Protein abundance profiling of the Escherichia coli cytosol, BMC Genom. 9 (2008) 102.
[34] W.L. Hubbell, H.M. McConnell, Molecular motion in spin-labeled phospholipids and membranes, J. Am. Chem. Soc. 93 (2) (1971) 314–326.
[35] T. Strohaker, et al., Structural heterogeneity of alpha-synuclein fibrils amplified from patient brain extracts, Nat. Commun. 10 (1) (2019) 5535.
[36] N. Van Eps, et al., Conformational equilibria of light-activated rhodopsin in nanodiscs, Proc. Natl. Acad. Sci. U. S. A. 114 (16) (2017) E3268–E3275.
[37] H. Sanabria, et al., Resolving dynamics and function of transient states in single enzyme molecules, Nat. Commun. 11 (1) (2020) 1231.
[38] J.T. Paletta, et al., Synthesis and reduction kinetics of sterically shielded pyrrolidine nitroxides, Org. Lett. 14 (20) (2012) 5322–5325.
[39] A.P. Jagtap, et al., Sterically shielded spin labels for in-cell EPR spectroscopy:

analysis of stability in reducing environment, Free Radic. Res. 49 (1) (2015) 78–85.
[40] G. Karthikeyan, et al., A bioresistant nitroxide spin label for in-cell EPR spectroscopy: in vitro and in oocytes protein structural dynamics studies, Angew Chem. Int. Ed. Engl. 57 (5) (2018) 1366–1370.
[41] N. Fleck, et al., SLIM: a short-linked, highly redox-stable trityl label for high-sensitivity in-cell EPR distance measurements, Angew Chem. Int. Ed. Engl. 59 (24) (2020) 9767–9772.
[42] S. Stoll, A. Schweiger, EasySpin, a comprehensive software package for spectral simulation and analysis in EPR, J. Magn. Reson. 178 (1) (2006) 42–55.